Simplified fabrication of integrated microfluidic devices using fused deposition modeling 3D printing

Gaal, Gabriel; Mendes, Melissa; Pedroso de Almeida, T.; Piazzetta, Maria H.O.; Gobbi, Ângelo L.; Riul, Antonio; Rodrigues, Varlei

DOI
10.1016/j.snb.2016.10.110

Publication date
2017

Document Version
Final published version

Published in
Sensors and Actuators B: Chemical: international journal devoted to research and development of physical and chemical transducers

Citation (APA)
Gaal, G., Mendes, M., Pedroso de Almeida, T., Piazzetta, M. H. O., Gobbi, Â. L., Riul, A., & Rodrigues, V. (2017). Simplified fabrication of integrated microfluidic devices using fused deposition modeling 3D printing. *Sensors and Actuators B: Chemical: international journal devoted to research and development of physical and chemical transducers*, *242*, 35-40. https://doi.org/10.1016/j.snb.2016.10.110

Important note
To cite this publication, please use the final published version (if applicable).
Please check the document version above.

Sensors and Actuators B 242 (2017) 35–40

Contents lists available at ScienceDirect

Sensors and Actuators B: Chemical

journal homepage: www.elsevier.com/locate/snb

Simplified fabrication of integrated microfluidic devices using fused deposition modeling 3D printing

Gabriel Gaal[a], Melissa Mendes[a], Tiago P. de Almeida[b,c], Maria H.O. Piazzetta[d], Ângelo L. Gobbi[d], Antonio Riul Jr.[a], Varlei Rodrigues[a,*]

[a] Instituto de Física "Gleb Wataghin", State University of Campinas, 777 Sergio Buarque de Holanda, Campinas, SP 13083-859, Brazil
[b] Faculty of Food Engineering, State University of Campinas, 80 Monteiro Lobato, Campinas, SP 13083-862, Brazil
[c] Department of Biotechnology, Delft University of Technology, 136 Julianalaan, Delft 2628, BL, Netherlands
[d] Microfabrication Laboratory, Brazilian Nanotechnology Laboratory, CNPEM, 10000 Guiseppe Maximo Scolfaro, Campinas, SP 13083-970, Brazil

ARTICLE INFO

Article history:
Received 31 May 2016
Received in revised form
19 September 2016
Accepted 24 October 2016
Available online 9 November 2016

Keywords:
3D printing
Microfluidic
e-Tongue

ABSTRACT

Microfluidic devices based on polydimethylsiloxane shown a plethora of experimental possibilities due to good transparency, flexibility and ability to adhere reversibly and irreversibly to distinct materials. Though PDMS is a milestone in microfluidic developments, its cost and handling directed the field to search for new options. 3D printing technology nowadays starts a revolution offering materials and possibilities that can contribute positively to current methodologies. Here we explored the fused deposition modeling 3D printing technique to obtain integrated, transparent and sealed microchannels made with polylactic acid, a cheap alternative material to set up microfluidic systems. Using a home-made 3D printer, devices could be assembled in a simplified process, enabling the integration of different materials such as paper, glass, wire and polymers within the microchannel. To demonstrate the efficacy of this approach, a 3D-printed electronic tongue sensor was built, enabling the distinction of basic tastes below the human threshold.

1. Introduction

The preeminent control, manipulation and analysis of liquids at the submillimeter scale in microfluidic devices allowed the integration of research fields with emergent technologies such as lab-on-chips and organ-on-chips [1–3]. Microfluidics has a great potential to fulfill analytical and preclinical challenges in a cost-effective manner, with numerous applications based on polydimethylsiloxane (PDMS), a milestone in the field [4,2] due to its non-toxicity, optical transparency, gas permeability, chemical inertness, low surface energy and good weatherability [5]. Currently, there is a growing interest in 3D-printing research as it offers a broader range of materials and the ability to fabricate objects with complex architectures avoiding multi-step processing.

The main 3D set up processes are stereolithography (SLA), fused deposition modeling (FDM), selective laser sintering (SLS), and direct ink writing (inkjet) [3,6], making the technique suitable across diverse applications. Some advantages of 3D printing for the microfluidic field are its simplicity, fast and efficient prototyping [3,7] with no need of photomasks, photoresists and clean room facilities. It can be straightforwardly replicated by non-expert users to build intricate structures at micrometer resolution, without the intensive, expensive and tiresome processes required by current techniques (soft-lithography, laser ablation, micromachining, etc). The FDM method enables the use of cost-effective thermoplastics such as polylactic acid (PLA), acrylonitrile butadiene styrene (ABS), polyethylene terephthalate (PET), nylon [8] and PLA-based conductive graphene filament, amenable to mass production [9].

PLA was chosen here as it is a well-established filament for FDM 3D-printers ensuring good reproducibility and a ready-to-use material for device fabrication. It is a thermoplastic composed by a linear aliphatic polyester chain synthesized from renewable resources, soluble in tetrahydrofuran, chlorinated solvents, hot benzene and dioxane [10], naturally biodegradable, lasting from six months to two years in the environment and it is also harmless if hydrolyzed, facilitating its final disposal [11,10,12–14]. Moreover, it is mechanically rigid with a relative high tensile strength (~50 MPa), maintaining its structural integrity upon 200 °C, an important feature in low temperature sterilization processes for implantable devices [15,10,16,17]. It is also chemically resistant in acidic media, allowing reversible surface functionalization with other polymers, coating with proteins and enzymes, or permanent

* Corresponding author.
E-mail address: varlei@ifi.unicamp.br (V. Rodrigues).

http://dx.doi.org/10.1016/j.snb.2016.10.110
0925-4005/

linkage with functional molecules in order to enhance biosensing response [18,17].

Comparatively, PDMS is more expensive than PLA and it presents some drawbacks such as low elastic modulus, which can cause geometric deformation in microfluidic structures under high pressure operation. Moreover, small molecules can be absorbed into PDMS structure, it is also vapor-permeable and it has a poor chemical compatibility with many organic compounds making it suitable mainly for aqueous applications. Finally, prototyping processes with PDMS require several steps, such as casting, curing, cooling, de-lamination and bonding, with an estimated processing time of 3 h [5,19].

The potential of 3D printing in microfluidics was already illustrated in previous reported works. A 3D printer was used to produce valve channels with distinct widths, heights and distances [20]. Begolo et al. 3D printed pumping lids to generate positive and negative pressures in a PDMS microfluidic device, allowing fast prototyping and design iterations without reducing the quality for portable diagnostics setups [21]. Interconnect channels with gasket-type seals punched into PDMS are prone to leak easily; however, Paydar and colleagues successfully 3D printed complex structures for customizable interconnect microfluidics [22]. 3D printed molds have been used for rapid fabrication and precise control of complex 3D channel geometries in PDMS, in fact many developments are still devoted in molding aimed for PDMS applications. Hwang and colleagues used 3D printed molds for precise control of complex 3D channel geometries in PDMS [23]. Moreover, Erkal et al. 3D printed microchannels that can be easily integrated with external electrodes for electrochemical detection [4]. Shallan et al. demonstrated the fabrication process of a complex, three-dimensional microfluidic device using stereolithography in less than 5 h [9].

We explore here the FDM 3D-priting technology to fabricate microchannels using PLA as an alternative material to PDMS, allowing a cost-effective and flexible technique to accelerate customized developments of microfluidic devices [3,24,5]. We show a simplified process to fabricate closed PLA microchannels monolithically integrated with other materials and successfully incorporated in practical devices. To illustrate the fabrication process and as proof-of-concept, a 3D-printed electronic tongue (e-tongue) was built and characterized to distinguish tastants below the human threshold.

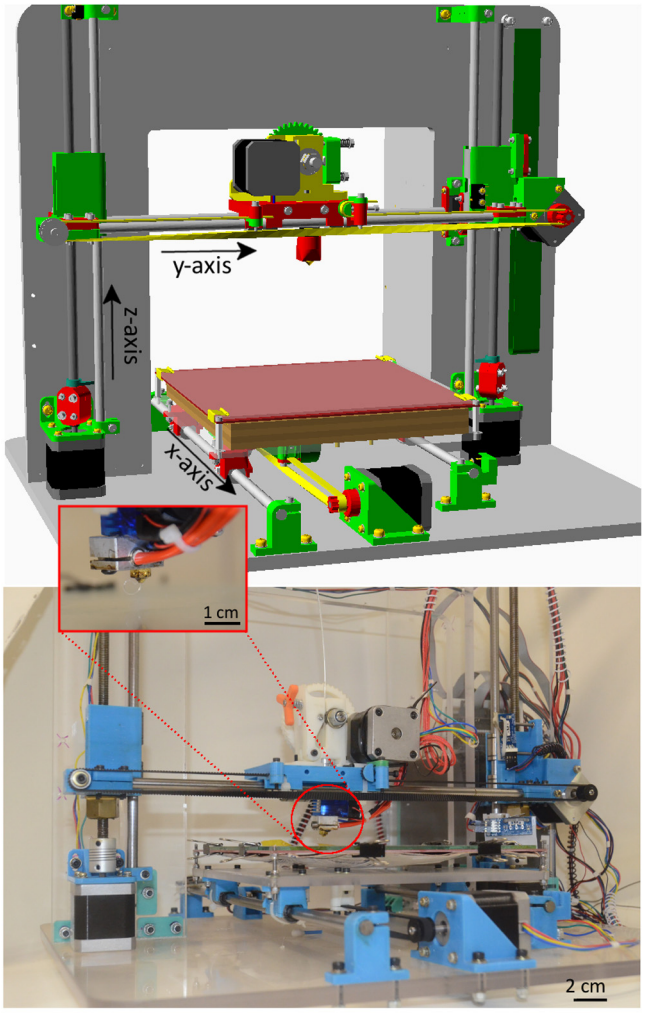

Fig. 1. (a) Prusa Mendel90 3D printer scheme from the open hardware RepRap project [25,26]. (b) Home-made built setup. Inset: 0.4 mm in diameter hot nozzle.

2. Experimental methods

2.1. 3D-printing setup

In this work we used a home-made 3D printer, based on the RepRap open hardware project [25]. In particular, a standard Prusa Mendel90 FDM 3D printer [26] was built, shown in Fig. 1. It uses a commercial hot nozzle of 0.4 mm in diameter for thermoplastics filaments of 1.75 mm in diameter, purchased from e3D [27]. The extruded thermoplastic is deposited on a hot table, which ensures the adhesion of the first layer and maintains a temperature gradient along the printing object, preventing delamination, i.e. separation of deposited layers from each other. Extruder and hot table are moved by stepper motors following Cartesian coordinates, printing the object in the layer-by-layer process. It was used a standard hot bed with 200 mm × 200 mm of building area, which allows the printing of multiples devices at the same time, using a mirror on the heated platen to ensure a flat and smooth printing surface. The PLA filament used to print the microchannels was also purchased from e3D [27], extruded at 200 °C, with the hot bed kept at 60 °C along the entire printing process. The printer was controlled by an open source arduino microcontroller board Mega 2560, interfaced with a commercial RepRap Arduino Mega Pololu Shield (RAMPS). Autodesk Inventor 2015 Student Edition was used to design 3D device models, which were further converted to a STereoLithography (STL) format [8]. Then the STL file was sliced by the free license software Slic3r that converts the 3D model into stacks of 2D printing planes [28]. Each plane contains a set of Cartesian coordinates that specify the amount and where the filament should be deposited using the G-code CNC language [8,29].

2.2. Microchannels characterization

The roughness of the microchannel (bottom, top and side walls) was an initial concern because the printer deposits molten thermoplastic threads side by side to make a layer. A perfilometer Dektak 150 was used to measure the roughness of the bottom part of an unsealed channel having 1200 μm in width and 400 μm in height. In order to show that the channel roughness does not generate instabilities to the flow and to verify the efficacy of the sealing by the 3D-printing process, a digital camera Nikon D7000 was used to record the flow through a three-inlet microchannel. Two different solutions prepared with red and green dyes, acquired in a local supermarket, were injected into the inlets. The RGB color components of the solutions was used to track the liquids through the main microchannel, checking for indications of mixture of the fluids.

Table 1
Parameters used in the LbL assembly of the materials to set up 3 e-tongue unit sensing.

#	Material	Concentration	pH	Deposition time (min)	Number of bilayers
1	PDDA	10 μL/mL	3.5	10	3
	GPSS	0.1 mg/mL	3.5	15	
2	PDDA	10 μL/mL	8.0	10	3
	CuTsPc	0.5 mg/mL	8.0	8	
3	PDDA	10 μL/mL	2.7	10	3
	MMT-K	1.0 mg/mL	2.7	10	

2.3. 3D-printed device

To demonstrate the efficiency of the 3D-printing process in fabricate a microfluidic device with integrated functionality, a microfluidic electronic tongue was built similar to that reported by Daikuzono et al. [30]. Briefly, the impedance is measured among coplanar, gold interdigitated electrodes (IDEs) coated with nanostructured films deposited by the layer-by-layer (LbL) technique onto the IDEs [31]. Poly(diallyldimethylammonium chloride) (PDDA) was used as cationic layer and either poly(styrenesulfonic acid) sodium salt (GPSS) [32], copper (II) phthalocyanine-tetrasulfonic acid tetrasodium salt (CuTsPc) or potassium montmorillonite (MMt-K) were used as the anionic layer. Finally, the device is established by integrating the 4 individual sensing units: bare IDEs and three other electrodes having 3-bilayer films of (PDDA/GPSS), (PDDA/CuTsPc) and (PDDA/MMt-K). The deposition parameters used in the LbL films formation are specified in Table 1 [30,33].

Gold IDEs were evaporated onto a transparency sheet to enable an irreversible bonding with the 3D-printed PLA microchannel. The IDES were fabricated at LNNano (Campinas, Brazil) and consisted of 30 pairs of fingers 3.6 mm long, having 40 μm in width and separated 40 μm each other (cell constant ~13.7 mm). The PLA microchannel had 600 μm in width and height, with a square chamber having the same height and 5 mm in width, designed to accommodate the active area of the IDEs, increasing the electrodes contact with the analyte. The inlet/outlet cylindrical structures were designed to fit the plastic hollow body of a common cotton swab. We also integrated a silicone hose to the other end of the rigid tube to facilitate the external connection with a syringe. Fig. 2 illustrates the 3D printed e-tongue, highlighting the place were the IDEs were inserted. It also shows the four sensing units comprising the microfluidic e-tongue system used to distinguish the tastants.

All solutions reported here were prepared using ultrapure water acquired from an Arium ® comfort Sartorius system. The samples analyzed with the 3D-printed e-tongue were prepared at 1 mM, using NaCl, HCl, caffeine and sucrose purchased from Sigma. Electrical response of the analytes were acquired using the impedance analyzer Solartron 1260A with Dielectric Interface 1269A. The solutions were driven through the sensing units using a syringe pump (New Era). Three independent sets of measurements were acquired at 6 kHz, with data analyzed using principal component analysis (PCA). According to the literature [30], at the kHz region the film/electrode interface rules the impedance of the system.

3. Results and discussion

3.1. Microchannel 3D printing

Our first challenge in using the FDM 3D printing technique was to print an open microchannel in PLA for further sealing with glass, paper or polymers, similar to the process usually made with PDMS. Leakages were always present due to the rough upper edges on the top channel surface, precluding a proper sealing. These difficulties were overtaken using PLA deposition itself to seal the microchannel, reducing the total time and steps involved for the device fabrication. Our strategy was to print first the ceiling on the hot bed, followed by the microchannel wall and its bottom. With this approach, careful adjustments to the printer and Slic3r settings were needed to avoid a collapse of the structure or the formation of net like structure at the first layer of the 3D-printed object, hampering future developments. The distance between the nozzle and the hot bed surface is a crucial parameter for the FDM technique because it cannot be too large, otherwise the molten filament does not adhere to the hot bed, and it cannot be too small since extrusion would be impeded. After a manual adjustment of the distance between the nozzle and the hot bed for an usual print, it was added a 0.1 mm negative offset on this distance compressing the first layer, thus creating an overlay among the printed tracks, ensuring a good sealing of the device. It is worth mentioning that this technique also increases the transparency of the first layer deposited, generating a clear window to observe the flow inside the 3D-printed microchannel.

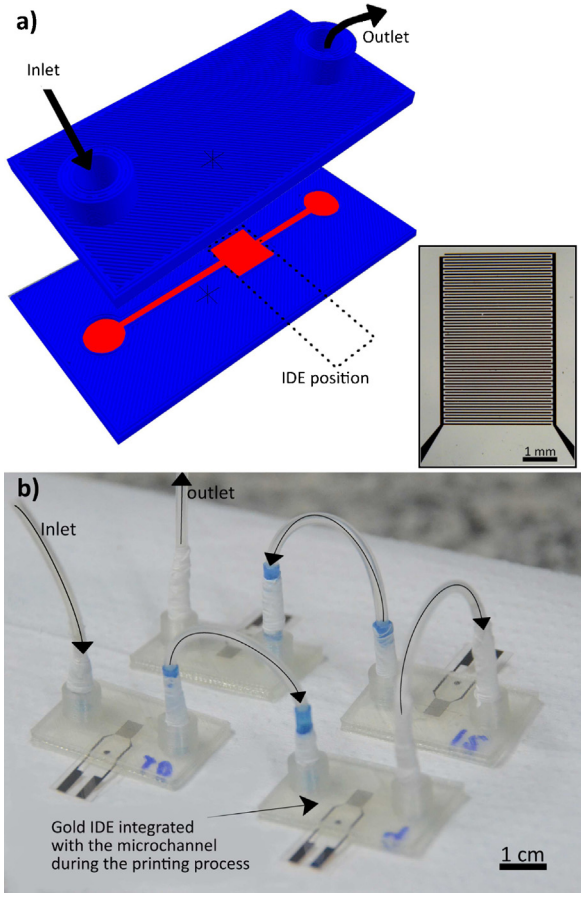

Fig. 2. (a) 3D model of the e-tongue with the microchannel in red. The gold IDEs were, manually inserted at the forth layer during the printing process at the outlined site; (b) e-tongues system. (For interpretation of the references to color in this figure legend, the reader is referred to the web version of this article.)

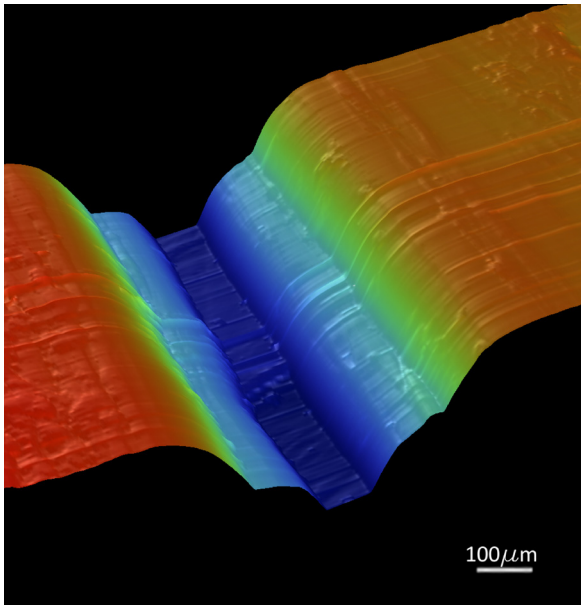

Fig. 3. Cross-section perfilometry of an opened 3D printed PLA microchannel.

This relative height, optimized to ensure both microchannel sealing and good transparency at the bottom part, introduced a distortion in the cross-section of the channel, illustrated in Fig. 3. The hot end nozzle exerts an extra pressure on the former deposited layers forcing them aside, which generates the observed v-shaped profile inside the microchannel. As a consequence, the channel dimensions are different from the 3D model, introducing up to 90% deviation from the nominal value on the first layer of the microchannel wall. Perfilometry analyses indicated a surface roughness of 2 μm on the printed tracks and 40 μm roughness due to the overlay of the tracks.

Despite the micrometer scale of the microchannel and its low Reynolds number (~1 in this work), the relative high surface roughness of the walls can introduce instabilities in the flow regime, acting as a passive microfluidic mixer, inherent to geometry of the microchannel [34]. This feature would be deleterious to various chemical and biochemical applications [35–39]. A three-inlet microchannel, 1200 μm in width was printed to verify both the influence of channel roughness and the "v-shaped" cross section on the flow regime. A red dye solution was pumped between two green dye solutions to facilitate RGB profile analyses, as shown in Fig. 4. The same flow rate was kept for the 3 inlets (1000 μL/h), a typical value for microfluidic applications. We defined the red and green signatures as the mean value of the pixels color of the regions 2 and 3 respectively, as presented in Fig. 4a. Fig. 4b shows the average value of the components of the red and green colors through the region 1 (Fig. 4a) and it indicates that the green and red dyes solutions in the main microchannel were unmixed. Therefore, the channel roughness did not introduce instabilities to the flow through the channel length (1.8 cm). Looking close to the Fig. 4b one can notice that the green signal starts to grow before the channel wall, leading to a misinterpretation that the microchannel is leaking to the sides. However, this feature is due a distortion in Fig. 4a, introduced by the tracks overlay.

3.2. Integrate substrates into the microchannel

Some microfluidic devices require the integration of different substrates inside the microchannel. After surpassing sealing problems reported here previously, paper, wires, glass, polymers and electrodes were successfully integrated into the 3D printed PLA

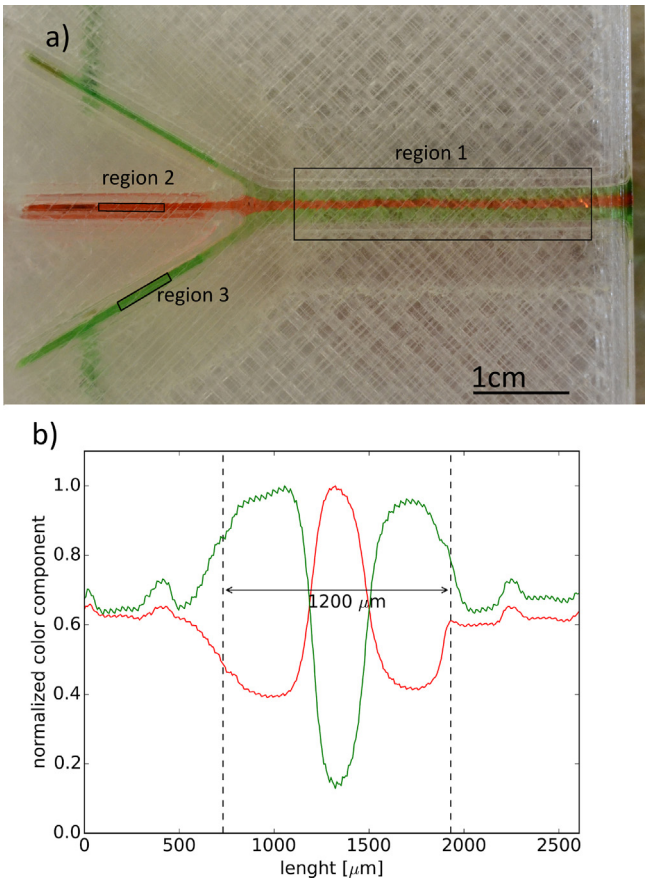

Fig. 4. (a) Laminar flow of dye solutions inserted in a three inlet microchip. Note the rectilinear infill with 20% fill, a grid, inside the body of the device. Regions 2 and 3 were used to define the red and green color components respectively, as the mean value of the pixels color. (b) Signature in region 1 of the colors defined on regions 2 and 3. It represents an average of the color intensity profiles transversal to the channel cross section. Dashed lines indicates the microchannel wall position. (For interpretation of the references to color in this figure legend, the reader is referred to the web version of this article.)

microchannel setup, as illustrated in Fig. 5. To accomplish that, we modified the original G-code and introduced a command to pause the printing process in a particular plane [29]. The desired material was then manually inserted, aligned with the microchannel and fixed with a high temperature polyimide tape to avoid a possible misalignment caused by the hot nozzle when the printing process was resumed. It is worth mentioning that in this work only thin materials were integrated into the microchannel, avoiding the need to adjust the 3D model to accommodate the inserted material. However, if the desired substrate is thicker than the printed layer height (in our set up ~200 μm) further adjustments to the project will be required to avoid a collision between the hot nozzle and the material inserted.

The FDM 3D printing technique can capitalize strengths and enhance the capability of the designers to improve analytical devices already developed and fabricate fully functional chips using non-expensive materials and methods. The tip-pinch posture offered by the FDM printing to integrate different materials can expand the microfluidic field as there is no need of tedious alignments, besides the fact that reaction zones can be integrated into different architectures and additional complex processing steps.

3.3. Microfluidic electronic tongue

To demonstrate the easy integration process of the FDM 3D printed, a proof-of-concept microfluidic electronic tongue system

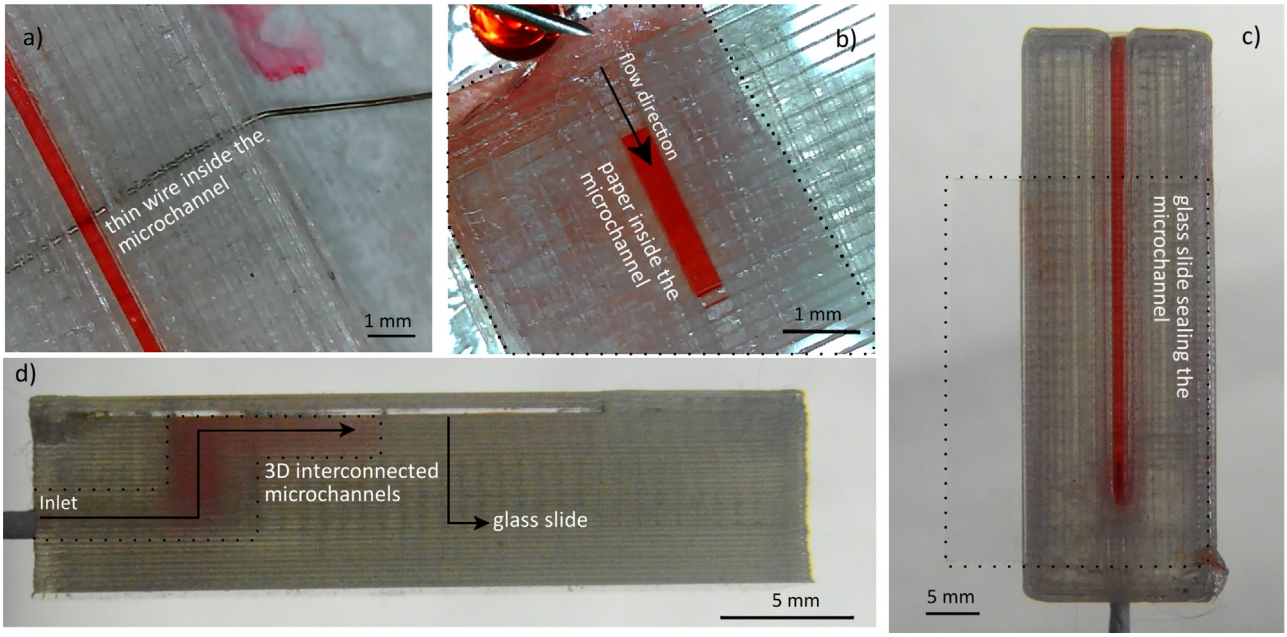

Fig. 5. Easy integration of materials during the 3D printing process expanding applications for multiple functionalities: (a) thin electrode integrated into the microchannel without leakage or flow obstruction; (b) flow driven by paper inserted into the microchannel; (c) glass slide introduced without leakage; (d) side view of (c) showing the 3D integration between channels placed in different heights.

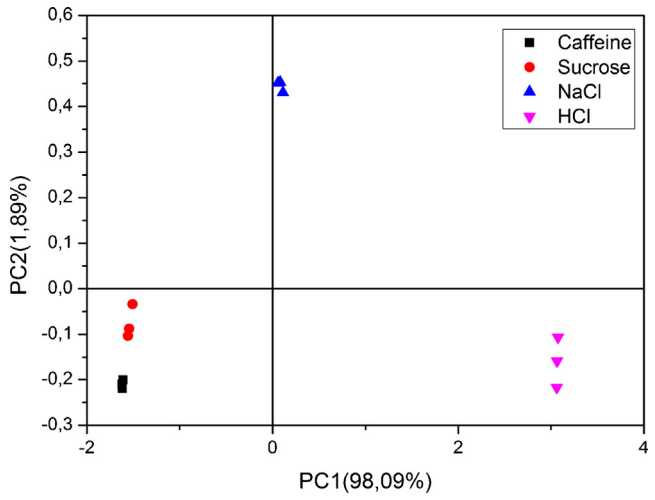

Fig. 6. PCA score plot for basic taste aqueous solutions prepared at 1 mM in three independent set of measurements. Sucrose (sweetness), NaCl (saltness), HCl (sourness) and caffeine (bitterness).

was developed as shown in Fig. 2. Solutions having basic tastes were pumped in the microchannels at 1000 μL/h with impedance data acquired when the liquid samples flow through the sensing units [30]. The distinct electrical behavior of the materials comprising the sensing units forms a fingerprint of the solutions analyzed, allowing for the distinction of the analytes [40]. The global response of the sensor was pooled in a PCA score plot, as shown in Fig. 6.

Briefly, PCA is a statistical method largely employed in multivariate analysis to reduce the dimensionality of the original data without losing information. It transforms the original dataset in uncorrelated variables called principal components that are obtained from a linear combination of the original variables. The first principal component (PC1) renders the highest variance of the measured variables, the second principal component (PC2) explains the maximum of the residual variance, and so on [41].

A good correlation of the tastants was reached (PC1 + PC2 = 99,98%), even considering salt and sweet solutions below the human threshold (10 mM for humans) [42]. As expected, a small dispersion of the data in three independent sets of measurements was observed, similarly to that reported by Daikuzono et al. [30], and a good distinction of the basic tastes was achieved, especially considering experimental difficulties to measure sucrose (non-electrolyte) and caffeine (hydrophobic solute in aqueous solution) [43,44].

4. Conclusions

We were able to 3D-print transparent and sealed PLA microchannels despite limitations in resolution imposed by the FDM technology. Important achievements included good transparency, printing of microchannels without collapsed structures, use of a cheap and more accessible material (PLA) alternative to PDMS and easy integration of other materials during printing. As a proof-of-concept, flexible interdigitated electrodes were easily incorporated in a microfluidic e-tongue capable of distinguishing basic tastes. Apart from using only microliters of the samples, it is important to stress the fact that this 3D-printed microfluidic e-tongue was built within less than one hour, something hard to achieve by traditional PDMS techniques. In summary, the 3D printing technology potentiates the field with more creative ideas, cost-effective and alternative materials for a rapid prototyping of complex structures as well as greater flexibility in design, paving the way to more abundant developments. The ability to readily change design and use materials other than PDMS demonstrated here will undoubtedly inspire future microfluidic integrations. The potential to print functional modules will also impact forthcoming developments in sensor applications made by non-experts, interdisciplinary expanding potentials and competences.

Acknowledgements

Authors are grateful to FAPESP (2014/03691-7), CNPq and CAPES for financial support. They also thank Prof. Osvaldo N. Oliveira Jr for

kindly revise the manuscript, the technician Vladimir Gaal and the engineer Antonio Carlos Costa, for useful discussions and support given in some experiments.

References

[1] E.W. Esch, A. Bahinski, D. Huh, Organs-on-chips at the frontiers of drug discovery, Nat. Rev. Drug Discov. 14 (4) (2015) 248–260, http://dx.doi.org/10.1038/nrd4539.

[2] E.K. Sackmann, A.L. Fulton, D.J. Beebe, The present and future role of microfluidics in biomedical research, Nature 507 (7491) (2014) 181–189, http://dx.doi.org/10.1038/nature13118.

[3] C. Meng, B. Ho, S.H. Ng, K. Ho, H. Li, Y.-J. Yoon, 3D printed microfluidics for biological applications, Lab Chip 15 (May) (2015) 3627–3637, http://dx.doi.org/10.1039/C5LC00685F.

[4] J.L. Erkal, A. Selimovic, B.C. Gross, S.Y. Lockwood, E.L. Walton, S. Mcnamara, R. Scott, D.M. Spence, 3D printed microfluidic devices with integrated versatile and reusable electrodes, Lab Chip 14 (2014) 2023–2032, http://dx.doi.org/10.1039/c4lc00171k.

[5] A.K. Au, N. Bhattacharjee, L.F. Horowitz, T.C. Chang, 3D-printed microfluidic automation, Lab Chip 15 (2015) 1934–1941, http://dx.doi.org/10.1039/C5LC00126A.

[6] J. Li, F. Rossignol, J. Macdonald, Inkjet printing for biosensor fabrication: combining chemistry and technology for advanced manufacturing, Lab Chip 15 (12) (2015) 2538–2558, http://dx.doi.org/10.1039/C5LC00235D.

[7] A. Waldbaur, H. Rapp, K. Lange, B.E. Rapp, Let there be chip – towards rapid prototyping of microfluidic devices: one-step manufacturing processes, Anal. Methods 3 (12) (2011) 2663–2954, http://dx.doi.org/10.1039/c1ay05253e.

[8] E. Canessa, C. Fonda, M. Zennaro, Low-Cost 3D Printing, 2013.

[9] A.I. Shallan, P. Smejkal, M. Corban, R.M. Guijt, M.C. Breadmore, Cost-effective three-dimensional printing of visibly transparent microchips within minutes, Anal. Chem. 86 (6) (2014) 3124–3130, http://dx.doi.org/10.1021/ac4041857.

[10] D. Garlotta, A literature review of poly(lactic acid), J. Polym. Environ. 9 (2) (2001) 63.

[11] A. Bhatia, R.K. Gupta, S.N. Bhattacharya, H.J. Choi, Compatibility of biodegradable poly(lactic acid) (PLA) and poly(butylene succinate) (PBS) blends for packaging application, Korea-Aust. Rheol. J. 19 (3) (2007) 125–131.

[12] Y. Tokiwa, B.P. Calabia, C.U. Ugwu, S. Aiba, Biodegradability of plastics bio-plastics, Int. J. Mol. Sci. 10 (2009) 3722–3742, http://dx.doi.org/10.3390/ijms10093722.

[13] Y. Rudeekit, J. Numnoi, M. Tajan, P. Chaiwutthinan, T. Leejarkpai, Determining biodegradability of polylactic acid under different environments, J. Met. Mater. Miner. 18 (2) (2008) 83–87.

[14] J.M. Anderson, M.S. Shive, Biodegradation and biocompatibility of PLA and PLGA microspheres, Adv. Drug Deliv. Rev. 28 (1997) 5–24.

[15] T.M. Rankin, N.A. Giovinco, D.J. Cucher, G. Watts, B. Hurwitz, D.G. Armstrong, Three-dimensional printing surgical instruments: are we there yet? J. Surg. Res. 189 (2) (2014) 193–197, http://dx.doi.org/10.1016/j.jss.2014.02.020.

[16] T. Patrício, M. Domingos, A. Gloria, P. Bártolo, Fabrication and characterisation of PCL and PCL/PLA scaffolds for tissue engineering, Procedia CIRP 5 (2013) 110–114, http://dx.doi.org/10.1016/j.procir.2013.01.022.

[17] M. Heiny, J.J. Wurth, V.P. Shastri, Chapter 9 – progress in functionalized biodegradable polyesters, in: S.G. Kumbar, C.T. Laurencin, M. Deng (Eds.), Natural and Synthetic Biomedical Polymers, Elsevier, Oxford, 2014, pp. 167–180, http://dx.doi.org/10.1016/B978-0-12-396983-5.00009-0.

[18] F. Carosio, S. Colonna, A. Fina, G. Rydzek, J. Hemmerle, P. Schaaf, F. Boulmedais, Efficient gas and water vapor barrier properties of thin poly(lactic acid) packaging films: functionalization with moisture resistant nafion and clay multilayers, Chem. Mater. 26 (2014) 5459–5466.

[19] H. Wang, D. Gao, Y. Meng, H. Wang, E. Wang, Y. Zhu, Corrosion-resistance, robust and wear-durable highly amphiphobic polymer based composite coating via a simple spraying approach, Prog. Org. Coat. 82 (2015) 74–80, http://dx.doi.org/10.1016/j.porgcoat.2015.01.012.

[20] J.L. Moore, A. Mccuiston, I. Mittendorf, R. Ottway, R.D. Johnson, Behavior of capillary valves in centrifugal microfluidic devices prepared by three-dimensional printing, Microfluid. Nanofluid. 10 (2011) 877–888, http://dx.doi.org/10.1007/s10404-010-0721-1.

[21] S. Begolo, D.V. Zhukov, D.A. Selck, L. Li, R.F. Ismagilov, The pumping lid: investigating multi-material 3D printing for equipment-free, programmable generation of positive and negative pressures for microfluidic applications, Lab Chip 14 (2014) 4616–4628, http://dx.doi.org/10.1039/C4LC00910J.

[22] O.H. Paydar, C.N. Paredes, Y. Hwang, J. Paz, N.B. Shah, R.N. Candler, Characterization of 3D-printed microfluidic chip interconnects with integrated O-rings, Sens. Actuators A: Phys. 205 (2014) 199–203, http://dx.doi.org/10.1016/j.sna.2013.11.005.

[23] Y. Hwang, O.H. Paydar, R.N. Candler, 3D printed molds for non-planar PDMS microfluidic channels, Sens. Actuators A: Phys. 226 (2015) 137–142, http://dx.doi.org/10.1016/j.sna.2015.02.028.

[24] P. Tseng, C. Murray, D. Kim, D.D. Carlo, Research highlights: printing the future of microfabrication, Lab Chip 14 (2014) 1491–1495, http://dx.doi.org/10.1039/c4lc90023e.

[25] http://reprap.org.

[26] http://hydraraptor.blogspot.com.br/2011/12/mendel90.html.

[27] http://e3d-online.com/.

[28] http://slic3r.org/.

[29] http://reprap.org/wiki/G-code.

[30] C.M. Daikuzono, C.A.R. Dantas, D. Volpati, C.J.L. Constantino, M.H.O. Piazzetta, A.L. Gobbi, D.M. Taylor, O.N. Oliveira, A. Riul Jr., Microfluidic electronic tongue, Sens. Actuators B: Chem. 207 (2015) 1129–1135, http://dx.doi.org/10.1016/j.snb.2014.09.112.

[31] G. Decher, Fuzzy nanoassemblies: toward layered polymeric multicomposites, Science 277 (5330) (1997) 1232–1237, http://dx.doi.org/10.1088/0957-4484/25/9/094006.

[32] W.S.J. Hummers, R.E. Offeman, Preparation of graphitic oxide, J. Am. Chem. Soc. 80 (1958) 1339.

[33] A. Riul Jr., D.S. Santos, K. Wohnrath, R.D. Tommazo, A.C.P.L.F. Carvalho, F.J. Fonseca, O.N. Oliveira, D.M. Taylor, L.H.C. Mattoso, Artificial taste sensor: efficient combination of sensors made from Langmuir–Blodgett films of conducting polymers and a ruthenium complex and self-assembled films of an azobenzene-containing polymer, Langmuir 18 (13) (2002) 239–245.

[34] C.-Y. Lee, C.-L. Chang, Y.-N. Wang, L.-M. Fu, Microfluidic mixing: a review, Int. J. Mol. Sci. (2011) 3263–3287, http://dx.doi.org/10.3390/ijms12053263.

[35] S. Takayama, E. Ostuni, P. LeDuc, K. Naruse, D.E. Ingber, G.M. Whitesides, Selective chemical treatment of cellular microdomains using multiple laminar streams, Chem. Biol. 10 (2) (2003) 123–130, http://dx.doi.org/10.1016/S1074-5521(03)00019-X.

[36] M. Tokeshi, T. Minagawa, T. Kitamori, Integration of a microextraction system on a glass chip: ion-pair solvent extraction of Fe(II) with 4,7-diphenyl-1,10-phenanthrolinedisulfonic acid and tri-n-octylmethylammonium chloride, Anal. Chem. 72 (7) (2000) 1711–1714, http://dx.doi.org/10.1021/ac991147f.

[37] J.P. Brody, P. Yager, R.E. Goldstein, R.H. Austin, Biotechnology at low Reynolds numbers, Biophys. J. 71 (December) (1996) 3430–3441.

[38] J.P. Brody, P. Yager, Diffusion-based extraction in a microfabricated device, Sens. Actuators A: Phys. 58 (1997) 13–18.

[39] M.N. Costa, B. Veigas, J.M. Jacob, D.S. Santos, J. Gomes, P.V. Baptista, R. Martins, J. Inácio, E. Fortunato, A low cost, safe, disposable, rapid and self-sustainable paper-based platform for diagnostic testing: lab-on-paper, Nanotechnology 094006 (24) (2014) 12, http://dx.doi.org/10.1088/0957-4484/25/9/094006.

[40] A. Riul Jr., C.A.R. Dantas, C.M. Miyazaki, O.N. Oliveira Jr., Recent advances in electronic tongues, Analyst 135 (10) (2010) 2481–2495, http://dx.doi.org/10.1039/c0an00292e.

[41] L.A. Berrueta, R.M. Alonso-Salces, K. Heberger, Supervised pattern recognition in food analysis, J. Chromatogr. A 1158 (2007) 196–214, http://dx.doi.org/10.1016/j.chroma.2007.05.024.

[42] J. Webb, D.P. Bolhuis, S. Cicerale, J.E. Hayes, R. Keast, The relationships between common measurements of taste function, Chemosens. Percept. 8 (2015) 11–18, http://dx.doi.org/10.1007/s12078-015-9183-x.

[43] B. Sharma, S. Paul, Understanding the role of temperature change and the presence of NaCl salts on caffeine aggregation in aqueous solution: from structural and thermodynamics point of view, J. Phys. Chem. B 119 (2015) 6421–6432, http://dx.doi.org/10.1021/jp512336n.

[44] T.H. Lilley, H. Linsdell, A. Maestre, Association-of caffeine in water and in aqueous solutions of sucrose, J. Chem. Soc. Faraday Trans. 88 (19) (1992) 2865–2870.